

# Gravitational waves in massive gravity theories: waveforms, fluxes and constraints from extreme-mass-ratio mergers

Vitor Cardoso,<sup>1,2,\*</sup> Gonçalo Castro,<sup>1,†</sup> and Andrea Maselli<sup>1,‡</sup>

<sup>1</sup>*Centro de Astrofísica e Gravitação - CENTRA, Departamento de Física,  
Instituto Superior Técnico - IST, Universidade de Lisboa - UL,  
Av. Rovisco Pais 1, 1049-001 Lisboa, Portugal*

<sup>2</sup>*Theoretical Physics Department, CERN, Geneva, Switzerland*

(Dated: April 1, 2025)

Is the graviton massless? This problem was addressed in the literature at a phenomenological level, using modified dispersion relations for gravitational waves, in linearized calculations around flat space. Here, we perform a detailed analysis of the gravitational waveform produced when a small particle plunges or inspirals into a large non-spinning black hole. Our results should presumably also describe the gravitational collapse to black holes and explosive events such as supernovae. In the context of a well-posed theory with massive gravitons and screening, merging objects up to 1 Gpc away or collapsing stars in the nearby galaxy may be used to constrain the mass of the graviton to be smaller than  $\sim 10^{-23}$  eV, with low-frequency detectors. Our results suggest that the absence of dipolar gravitational waves from black hole binaries may be used to rule out entirely such theories.

## I. INTRODUCTION

General Relativity (GR) is special and unique, in a very precise mathematical sense [1, 2]. Nevertheless, several arguments suggest that such an elegant theory cannot easily accommodate neither the ultraviolet nor the infrared description of the universe. Simultaneously, observations of large-scale phenomena indicate that either the matter sector or the gravitational interaction require a better understanding. In other words, extensions of GR are welcome. One of the possible extensions draws inspiration from the standard model of particle physics, and consists in allowing for a massive graviton [2–4].

Bounds on such theories can be imposed via gravitational-wave (GW) emission and propagation mechanisms. These include:

- i. modified dispersion relations for GWs, *assuming* that the generation of these waves is as in GR [5].
- ii. The spin-down of black holes (BHs), caused by superradiant instabilities [6].
- iii. Changes in the orbital period of binary pulsars, caused by a different energy flux [7].

There are no constraints using directly the measured properties of GWs, without any assumption on the production mechanism. Our main concern here is precisely to compute the gravitational waveform and fluxes from the merger of two compact objects, using the strong-field regime of massive gravity theories. We consider the ghost-free theory describing two interacting spin-2 fields described in Appendix A. This theory admits the

same BH solutions as GR. We therefore investigate how BHs in massive gravity theories respond dynamically. In particular, we consider mergers of extreme-mass ratio objects in which the massive one is a Schwarzschild BH. Our results are very generic, but we focus on the truly unique features of massive gravity theories: the extra polarizations with respect to GR. The calculations can, in principle, encompass also collapsing objects as long as the final state is a BH. Finally, the extrapolation to nearly-equal mass objects allows us to infer physics of interest to Earth-based detectors.

Throughout this work we use geometrized units, in which  $G = c = 1$ .

## II. FORMALISM AND MASTER EQUATIONS

In our framework, a small point particle is orbiting, or merging with, a massive Schwarzschild BH of mass  $M$ . This system may model the merger of a neutron star with a stellar-mass or a supermassive BH, but it may well describe qualitatively the merger of two equal-mass BHs as well. In fact, the lesson from the two-body problem in GR is that perturbation theory is able to account for this process even at a quantitative level [8]. The point particle moves on a spacetime geodesic  $y_p^\mu(\tau) = (t_p(\tau), r_p(\tau), \theta_p(\tau), \varphi_p(\tau))$ , with  $\tau$  being the test body proper time. The particle is taken to be pointlike and described by the stress-energy tensor

$$T^{\mu\nu} = m_p \int (-g)^{1/2} u^\mu u^\nu \delta^{(4)}(x^\beta - y_p^\beta) d\tau , \quad (1)$$

where  $m_p$  is the rest mass of the test particle and  $u^\mu = dy_p^\mu/d\tau$  its 4-velocity. The point particle stress slightly disturbs the background ge-

\* [vitor.cardoso@tecnico.ulisboa.pt](mailto:vitor.cardoso@tecnico.ulisboa.pt)

† [gcabritac@gmail.com](mailto:gcabritac@gmail.com)

‡ [andrea.maselli@tecnico.ulisboa.pt](mailto:andrea.maselli@tecnico.ulisboa.pt)

ometry  $\bar{g}_{\mu\nu}$ ,  $\bar{f}_{\mu\nu}$  (the theory has two metrics) describing the massive object and a graviton of mass  $\mu$ . Schematically, it contributes with fluctuations  $(\delta g_{\mu\nu}, \delta f_{\mu\nu})$ , which we analyse in tensor spherical harmonics and Fourier decompose. Details are left for the Appendices A–E (see also Ref. [6]).

### A. Head-on collisions

Hereafter, we consider two prototypical dynamical processes: radial infall corresponding to head-on collisions, and pure equatorial motion corresponding to quasicircular inspirals (once radiation reaction is taken into account). The complete expressions for the source components in these two specific configurations are shown in Appendix D. For radial motion, axial perturbations are not excited. The multipolar expansion then describes only polar-type perturbations with  $\ell \geq 0$ . Of these, the  $\ell \geq 2$  equations contain small  $\mu$ -dependent corrections to the GR expressions. We do not consider these any further<sup>1</sup> and focus on the truly unique properties of massive gravity: the presence of new degrees of freedom, described by the  $\ell = 0$  and  $\ell = 1$  modes.

For the monopole,  $\ell = 0$  mode, the number of perturbation functions reduces to the four metric components  $(H_0, H_1, H_2, K)$  (see Appendices and Ref. [6]). Through the following transformation:

$$K = \frac{\sqrt{-4\mu^2 M + \mu^4 r^3 + 2\mu^2 r + 4r\omega^2}}{r^{5/2}} \varphi_0, \quad (2)$$

we obtain a single wave equation for  $\varphi_0$ :

$$\frac{d^2\varphi_0}{dr_*^2} + [\omega^2 - V_{\text{pol}}^{\ell=0}(r, \omega)]\varphi_0 = \mathcal{S}_{\text{pol}}^{\ell=0}. \quad (3)$$

Here,  $V_{\text{pol}}^{\ell=0}(r, \omega)$  is a radial potential whose expression is lengthy and not very illuminating, while  $r_*$  is a tortoise coordinate defined by  $dr_*/dr = 1/f$ . The potential  $V_{\text{pol}}^{\ell=0}(r, \omega) \sim \mu^2$  at large spatial distances, and it vanishes close to the BH horizon. The source term  $\mathcal{S}_{\text{pol}}^{\ell=0}$  depends on the radial position and on the energy with which the point particle is colliding. In the highly relativistic regime,

$$\mathcal{S}_{\text{pol}}^{\ell=0} = \frac{8\sqrt{2}m_p\gamma(r-2M)(\mu^2r+2i\omega)e^{i\omega t_p(r)}}{\sqrt{r}(-4\mu^2M+\mu^4r^3+2\mu^2r+4r\omega^2)^{3/2}}, \quad (4)$$

where  $\gamma$  is the Lorentz boost factor of the test particle at large spatial separations. Note that the

$z$ -axis is chosen to coincide with the particle trajectory, hence only  $m = 0$  modes are excited.

For the dipole  $\ell = 1$  term the perturbations are completely determined by two coupled equations for  $K$  and  $\eta_1$ , which can be recast in a linear form as:

$$\left[ \frac{d}{dr_*} + V_{\text{pol}}^{\ell=1}(r) \right] \boldsymbol{\Sigma} = \mathcal{S}_{\text{pol}}^{\ell=1}, \quad (5)$$

where  $\boldsymbol{\Sigma} = (K, \eta_1, dK/dr_*, d\eta_1/dr_*)^T$ , and  $V_{\text{pol}}^{\ell=1}$  is a  $4 \times 4$  matrix which is shown within the supplementary material. For a radial infalling particle with a relativistic boost factor, the source vector is simply given by

$$\mathcal{S}_{\text{pol}}^{\ell=1} = (0, 0, S_K, S_{\eta_1}) = (0, 0, f(r)/r, 1)S_{\eta_1}, \quad (6)$$

where  $f(r) = (1 - 2M/r)$  and

$$S_{\eta_1} = -\frac{8\sqrt{6}m_p\gamma(2+r^2\mu^2+2ir\omega)e^{i\omega t_p(r)}}{4Mr^2\mu^2-8M-6r^3\mu^2-r^5\mu^4-4r^3\omega^2}. \quad (7)$$

### B. Quasi-circular inspirals

For circular motion, the only non-trivial new degree of freedom is the dipolar-polar component. Our system of equations can be written as

$$K'' + a_1 K' + a_2 K + a_3 \eta_1' + a_4 \eta_1 = S_1 \delta(r - r_p), \quad (8)$$

$$\eta_1'' + b_1 \eta_1' + b_2 \eta_1 + b_3 K' + b_4 K = S_2 \delta(r - r_p), \quad (9)$$

where primes stand for tortoise derivatives, and  $r_p$  is the orbital radius of the test particle. The system above can be cast in the form

$$\left[ \frac{d}{dr_*} + V_{\text{pol}}^{\ell=1}(r) \right] \boldsymbol{\Sigma} = \mathcal{S}_{\text{circ}}^{\ell=1}, \quad (10)$$

being  $\boldsymbol{\Sigma} = (K, \eta_1, dK/dr_*, d\eta_1/dr_*)^T$  and  $\mathcal{S}_{\text{circ}}^{\ell=1} = (0, 0, S_K^{\text{circ}}, S_{\eta_1}^{\text{circ}})$ . We solve eq. (10) by first constructing a  $4 \times 4$  fundamental matrix  $X$  built with the homogenous solutions of the previous system (see Appendix E), which yields the general solution:

$$\boldsymbol{\Sigma}(\omega, r) = X \int_{-\infty}^{\infty} X^{-1} \mathcal{S}_{\text{circ}}^{\ell=1} dr_*. \quad (11)$$

Note that the source vector contains a linear combinations of the Dirac delta and its first derivative. Therefore, integrating by part eq. (11) we can immediately obtain an explicit form for the metric functions,  $\boldsymbol{\Sigma}(\omega, r) = X[\mathbf{A} + \mathbf{B}]$ , where  $\mathbf{A}$  and  $\mathbf{B}$  are two vectors given by:

$$\mathbf{A} = \left( 1 - \frac{2M}{r_p} \right) X^{-1}(r_p) \mathcal{S}_{\text{circ}}^{\ell=1}(r_p), \quad (12a)$$

$$\mathbf{B} = -\frac{d}{dr} \left[ \left( 1 - \frac{2M}{r} \right) X^{-1} \mathcal{S}_{\text{circ}}^{\ell=1} \right]_{r=r_p}. \quad (12b)$$

<sup>1</sup> Such corrections were studied in some detail in the weak-field, slow-motion limit elsewhere [7].

### III. NUMERICAL RESULTS

In this section we describe the numerical results obtained by solving the systems of ODEs for the monopole and dipole component of the polar sector. As described in Sec. II, we consider circular and radial trajectories: for both the configurations, axial modes are not excited, as the source terms vanish. We integrate eq. (3) and eqns. (5) through a Green function approach, with appropriate boundary conditions at the BH horizon and at spatial infinity (see Appendix E for further details).

#### A. Head-on collisions

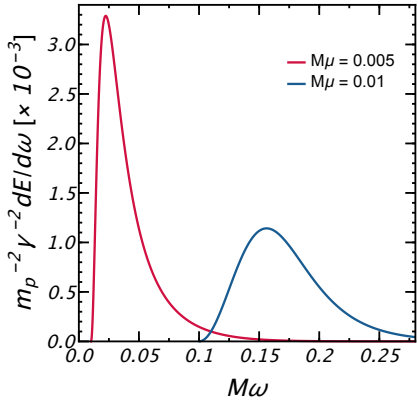


FIG. 1. GW energy spectrum  $dE/d\omega$  for the  $\ell = 0$  polar mode, with  $M\mu = (0.1, 0.01)$  and a radial infalling particle.

For head-on collisions, the waveform amplitude scales linearly with the mass of the infalling point particle, and the only free parameter is the relative velocity at large distances. We fix this to be relativistic, and we find, as expected, that the amplitude then scales linearly with the boost factor  $\gamma$ . Although our formalism includes the general case, relativistic collisions should mimic well the late stages of inspiral. In addition, and perhaps more important for us here, they should also describe even explosive events such as supernovae. In theories of massive gravity, even spherically symmetric explosive events release a non-negligible amount of radiation in the monopole mode.

The energy spectrum  $dE/d\omega$  for the monopole perturbation is shown in Fig. 1 as a function of the frequency  $\omega$ , for a head-on collision (see Appendix F for technical details). The spectrum peaks close to the value of the graviton mass, and quickly decays to zero for higher frequencies. The total integrated energy is not shown but it scales like

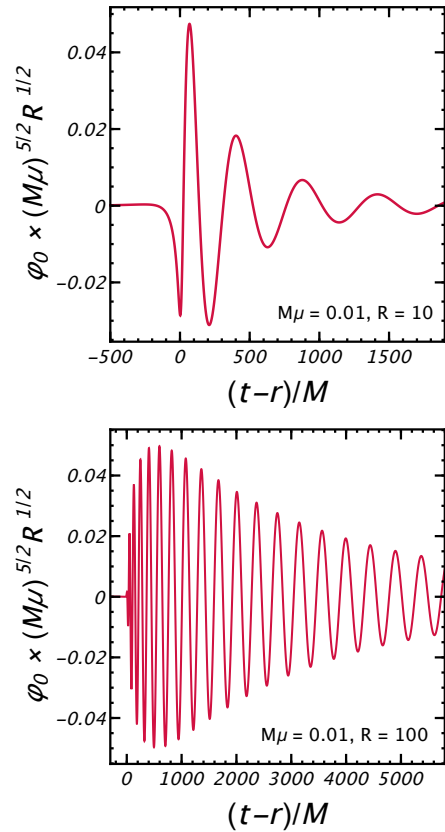


FIG. 2. Gravitational waveforms for the  $\ell = 0$  component of the polar sector, and a radial infalling particle, as a function of the retarded time  $(t - r)/M$ . We consider  $M\mu = 0.01$  and different extraction radius at  $R\mu = (10, 100)$ . The waveform scales trivially with the BH mass  $M$  and the particle mass and boost  $m_p, \gamma$ , according to eq. (14).

$E_{\text{tot}} \sim 0.01\mu m_p^2 \gamma^2$  at small couplings  $M\mu$ .

Knowing the solution in the frequency domain, we can immediately compute the GW signal as a function of the retarded time by simply applying a Fourier transform to  $\varphi_0(\omega)$ . This is shown in Fig. 2 for two values of the extraction radii  $R = r\mu = (10, 100)$ . It is important to highlight that GWs in theories of massive gravity are *dispersed*: the waveform at large distances is no longer a function only of  $t - r$ . This property is apparent in Fig. 2 and was also recently discussed in other setups [9]. We find that the peak of the (time-domain) waveform can be described by the following scaling,

$$\varphi_0^{\text{peak}} \sim \kappa \frac{m_p \gamma M^2}{(M\mu)^{5/2} R^{1/2}}, \quad (13)$$

where  $\kappa \simeq 0.055$ , when the extraction radius  $R > 1$ . This is not too surprising, given the  $\mu$ -dependence of the source term, eq. (7), at low frequencies  $\omega \sim \mu$ . Our results indicate that the peak

of the amplitude, with respect to the beginning of the signal, can be approximated by the following law,

$$(t-r)^{\text{peak}} \sim (M\mu)^{-0.34} MR$$

$$\sim 1800 \left( \frac{M}{M_\odot} \right)^{0.66} \left( \frac{\mu}{10^{-23} \text{eV}} \right)^{0.66} \frac{r}{8 \text{Kpc}} \text{secs.}$$

When expressed in terms of physical metric perturbations, we find

$$K^{\text{peak}} = \kappa \frac{m_p}{M} \left( \frac{M}{r} \right)^{3/2} \frac{1}{M\mu} \quad (14)$$

$$\sim 10^{-16} \frac{m_p \gamma}{0.01 M} \sqrt{\frac{M}{M_\odot}} \left( \frac{8 \text{Kpc}}{r} \right)^{3/2} \frac{10^{-23} \text{eV}}{\mu}$$

$$\sim 10^{-22} \frac{m_p \gamma}{0.01 M} \sqrt{\frac{M}{M_\odot}} \left( \frac{\text{Gpc}}{r} \right)^{3/2} \frac{10^{-25} \text{eV}}{\mu}.$$

These numbers are encouraging, however the large-amplitude signals carry a low-frequency content  $\omega \sim \mu$ , corresponding to a frequency [10]

$$f \sim 2.5 \times 10^{-9} \left( \frac{\mu}{10^{-23} \text{eV}} \right) \text{Hz.} \quad (15)$$

Thus, observations of these signals will require low-frequency sensitive detectors.

At late times and large extraction radii, the waveform is exponentially damped. We cannot rule out power-law decay at very late times. We have searched for the characteristic ringdown modes in this theory and find both good agreement with previously reported values [6] and with the ones inferred from the time-domain waveforms. We note in particular the presence of an unstable mode, which does not seem to be significantly excited - on these timescales. Waveforms for the  $\ell = 1$  mode are shown in Fig. 3 (again for relativistic collisions). The maximum value of the amplitudes can be described again with a scaling factor of the form given by eq. (13) (see caption of Fig. 3).

Our results can also be applied to spherically symmetric collapse: in such a case, the source term is trivially replaced by a spherically-symmetric shell; the final source term is unchanged. Even if 1% of the star's rest mass is involved in the collapse, our results indicate that the peak waveform is detectable when  $\mu$  is small enough. In fact, eq. (14) implies that stronger constraints can be obtained via (non-) observations of GWs from collapsing stars in our galaxy. Such conclusions are consistent also with recent results of core-collapse supernovae in massive scalar-tensor theories of gravity [9].

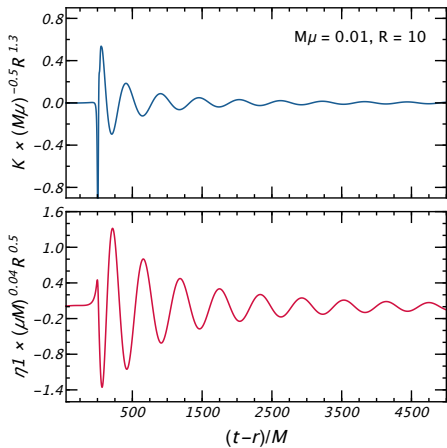


FIG. 3. Waveforms obtained for the  $\ell = 1$  polar mode, derived for a radial infalling particle with source term given by eq. (7), as a function of the retarded time  $(t-r)/M$ . The panel refers to  $M\mu = 0.01$  at extraction radii  $R\mu = 10$ . The overall behavior is the same as the monopole  $\ell = 0$  mode. The maximum amplitudes of the two metric functions scale as  $K^{\text{peak}} \sim m_p \gamma \delta_1 \sqrt{M\mu} / R^{1.3}$  and  $\eta_1^{\text{peak}} \sim m_p \gamma M \delta_2 (M\mu)^{-0.04} / R^{1/2}$  where  $(\delta_1, \delta_2) \simeq (0.84, 1.3)$  (these expressions also provide the scaling with  $M, m_p, \gamma$ ).

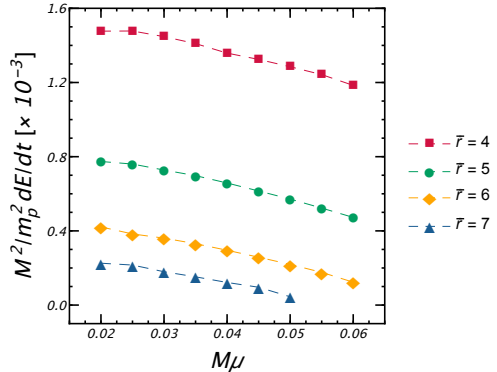


FIG. 4. GW luminosity  $dE/dt$  for the  $(\ell, m) = (1, 1)$  polar mode as a function of the 2-spin field mass  $M\mu$  for different radius  $\bar{r} = r_p/M$  of the test particle on circular orbits around the BH.

## B. Particles in circular motion

Quasi-circular inspirals in the weak-field, slow-motion approximation have been used to impose constraints on massive theories of gravity using pulsar timing observations [7]. Those constraints used only corrections - which scaled like  $\mu^2$  - to the quadrupole formula. Our results include relativistic motion in strong-gravity situations. In GR, particles in circular motion excite only quadrupolar or higher modes. As we saw, a new, dipolar mode arises in massive gravity, the energy flux of

which is shown in Fig. 4.

For a particle in a circular orbit of radius  $r_p$ , our results indicate that the flux in the  $\ell = m = 1$  mode scales like  $1/r_p^4$ , so truly a dipolar behavior, with BHs having a nontrivial dipolar charge in this theory. Furthermore, the charge is non-negligible at small  $M\mu$ . We find a flux  $dE/dt \sim 0.6m_p^2M^2/r_p^4$ . The quadrupole formula, on the other hand, predicts a quadrupolar emission  $dE/dt = (32/5)m_p^2M^3/r_p^5$ . This is one of our main results: the dipolar emission in massive gravity theories dominates the GR quadrupolar term, at arbitrarily small  $\mu$ . Thus, observations of binary BHs can potentially be used to rule out these theories [11].

#### IV. DISCUSSION

We have worked out the details of gravitational radiation in theories of massive gravity, when two BHs merge. It is clear that a substantial fraction of the radiation emitted in this process decays slowly, at large distances. In fact, because the graviton is massive, low-energy GWs are confined. This was also noticed in Ref. [9]. Such radiation will clearly have an impact in any star or object located within its sphere of influence, but such effects are unknown to us so far. Circular motion at an orbital frequency  $\omega = \mu$  will likely lead to resonant excitations of dipolar GWs. Unfortunately, the numerical study of such resonances is a challenging task [12–14], upon which we did not embark.

Technically, our procedure is free of computational challenges. The numerical results are converging and very clear: we show that new modes are excited to a substantial amplitude, both in head-on collisions and in quasi-circular motion. For head-on collisions – because new modes are excited at characteristically small frequencies – GW detectors sensitive to low frequency radiation will be able to impose constraints on the mass of gravitons tighter than ever before. In fact, if we trust that our results carry over to two, nearly equal-mass neutron stars, then the constraints on the mass of the graviton will be improved by two orders of magnitude or more. The dipolar mode excited by quasi-circular inspirals is in fact dominant with respect to the GR quadrupolar emission. Thus, accurate observations of binary BHs have the potential to tightly constraint massive gravity.

Alternatively, our results can be a manifestation that the background geometry does not describe astrophysical BHs. Indeed, it can be shown that Schwarzschild (and Kerr) BHs are unstable in theories with a massive graviton [6, 15, 16]. Nevertheless, for small mass coupling  $M\mu$  the instability timescale is extremely large and the spacetime re-

sponds to short-timescale phenomena “unaware” of the instability. Thus, sufficiently short-scale phenomena are expected to produce Schwarzschild BHs, and our methods and results apply in the regime where we would like them to, which is that of small graviton masses. In addition, numerical results suggest that when one of the metrics is taken to be non-dynamical, hairy stationary BHs do not even exist [16, 17]. One cannot exclude the possibility that a viable astrophysical BH is described by a dynamical metric [18], in which case our results could change considerably. Notwithstanding, it is clear that GW astronomy carries a huge potential to understand theories of massive gravity, but that several challenges (including the correct description of astrophysical BHs) needs to be seriously tackled.

#### ACKNOWLEDGMENTS

We are indebted to Claudia de Rham, Chris Moore and Andrew Tolley for many and very useful comments, discussions and suggestions. The authors acknowledge financial support provided under the European Union’s H2020 ERC Consolidator Grant “Matter and strong-field gravity: New frontiers in Einstein’s theory” grant agreement no. MaGRaTh-646597. This project has received funding from the European Union’s Horizon 2020 research and innovation programme under the Marie Skłodowska-Curie grant agreement No 690904. The authors would like to acknowledge networking support by the GWverse COST Action CA16104, “Black holes, gravitational waves and fundamental physics.”

#### Appendix A: Field equations

In the following sections we will provide the basic ingredients to compute, *ab initio*, the equations describing metric perturbations in the dRGT theory [19], which we then numerically integrate in Sec. III. The ghost-free action that describes two interacting spin-2 fields in vacuum is:

$$S = \int d^4x \sqrt{-g} \left[ M_g^2 R_g + \sqrt{\frac{f}{g}} M_f^2 R_f - 2M_v^4 V(g, f) \right] \quad (\text{A1})$$

where  $R_g$  and  $R_f$  are the Ricci scalars of the two metrics  $g_{\alpha\beta}$  and  $f_{\alpha\beta}$ , whose determinants are given by  $g$  and  $f$  [20]. The matter couplings in eq. (A1) are given by  $M_g^{-2} = 16\pi G$ ,  $M_f^{-2} = 16\pi G$ , and  $M_v$ . The latter can be expressed as a function of the first two. In the limit  $M_f \rightarrow 0$ , eq. (A1) reduces to a massive gravity theory in which matter

coupling and the kinetic term of  $f_{\mu\nu}$  vanish [21]. The two quantities  $f$  and  $g$  can be recast in terms of 5 interactions coefficients, free of the Boulware-Deser ghosts on generic backgrounds [19, 20, 22]. The potential  $V$  is given by:

$$V(\gamma, \beta_n) = \sum_{n=0}^4 \beta_n e_n(\gamma) , \quad (\text{A2})$$

where  $\beta_n$  are coupling constants, and  $e_n(\gamma)$  are symmetric polynomials of the matrix  $\gamma^\mu{}_\nu = \sqrt{g^{-1}} f^\mu{}_\nu$ , which can be written in 4 dimensions as:

$$\begin{aligned} e_0 &= 1 , & e_1 &= [\gamma] , & e_2 &= \frac{1}{2}([\gamma]^2 - [\gamma^2]) , \\ e_3 &= \frac{1}{6}([\gamma]^3 - 3[\gamma][\gamma^2] + 2[\gamma^3]) , & e_4 &= \det(\gamma) , \end{aligned}$$

where  $[\cdot]$  denotes the trace of the matrix. Varying the action (A1) with respect to  $g_{\mu\nu}$  and  $f_{\mu\nu}$  we obtain two sets of equations:

$$R_{\mu\nu}(g) - \frac{1}{2}g_{\mu\nu}R(g) + \frac{M_v^4}{M_g^2}V_{\mu\nu}^g = \frac{T_{\mu\nu}^g}{m_g^2} , \quad (\text{A3})$$

$$R_{\mu\nu}(f) - \frac{1}{2}f_{\mu\nu}R(f) + \frac{M_v^4}{M_f^2}V_{\mu\nu}^f = \frac{T_{\mu\nu}^f}{m_f^2} , \quad (\text{A4})$$

where the interactions terms  $V_{\mu\nu}^{f,g}$  depend on the matrix  $\gamma$ , and the stress-energy tensors are defined such as  $(T_{\mu\nu}^g, T_{\mu\nu}^f) = -\frac{1}{\sqrt{g}}(\frac{\delta S_m}{\delta g^{\mu\nu}}, \frac{\delta S_m}{\delta f^{\mu\nu}})$ .

Choosing the two metrics to be proportional [6, 23], i.e.  $\bar{f}_{\mu\nu} = c^2 \bar{g}_{\mu\nu}$ <sup>2</sup> eqns. (A3)-(A4) lead to two copies of the Einstein's equations for  $\bar{f}$  and  $\bar{g}$ :

$$\bar{R}_{\mu\nu} - \frac{1}{2}\bar{g}_{\mu\nu}\bar{R} + \bar{f}_{\mu\nu}\Lambda_g = \frac{T_{\mu\nu}^f}{m_g^2} , \quad (\text{A5})$$

$$\bar{R}_{\mu\nu} - \frac{1}{2}\bar{g}_{\mu\nu}\bar{R} + \bar{g}_{\mu\nu}\Lambda_g = \frac{T_{\mu\nu}^g}{m_g^2} . \quad (\text{A6})$$

Note that, consistency of the background relations requires  $\Lambda_g = \Lambda_f$ , and that the stress energy tensor are proportional through the matter couplings,  $T_{\mu\nu}^f = M_f^2/M_g^2 T_{\mu\nu}^g$ .

In this work we focus on BH solutions, with  $T_{\mu\nu}$  being a first order perturbation of the background metric, and explicitly given by eq. (1). We also assume that the cosmological constants vanish,  $\Lambda_f = \Lambda_g = 0$ , as their effect can be considered negligible on the scales relevant for the local physics around BHs. We can therefore consider asymptotically flat solutions. Equations (A5)-(A6), supplied

<sup>2</sup> Background quantities are identified by a bar superscript.

by usual ansatz for a spherically symmetric space-time with coordinates  $x^\mu = (t, \vec{x}) = (r, t, \theta, \varphi)$ :

$$ds^2 = -f(r)dt^2 + \frac{dr^2}{g(r)} + r^2d\theta^2 + r^2\sin^2\theta d\varphi^2 , \quad (\text{A7})$$

yield the Schwarzschild solution for a BH of mass  $M$ , with  $f(r) = g(r) = 1 - 2M/r$ .

We can now turn our attention on the metric perturbations. At the linear order we have:

$$g_{\mu\nu} = \bar{g}_{\mu\nu} + M_g^{-1}\delta g_{\mu\nu} , \quad (\text{A8})$$

$$f_{\mu\nu} = \bar{f}_{\mu\nu} + cM_f^{-1}\delta f_{\mu\nu} . \quad (\text{A9})$$

Although the functions  $\delta g_{\mu\nu}$  and  $\delta f_{\mu\nu}$  are generically independent, it is possible to find a suitable combination:

$$h_{\mu\nu}^{(0)} = \frac{M_g\delta g_{\mu\nu} + cM_f\delta f_{\mu\nu}}{\sqrt{c^2M_f^2 + M_g^2}} , \quad (\text{A10})$$

$$h_{\mu\nu} = \frac{M_g\delta f_{\mu\nu} - cM_f\delta g_{\mu\nu}}{\sqrt{c^2M_f^2 + M_g^2}} , \quad (\text{A11})$$

for which the perturbations decouple, yielding two sets of field's equations [20]. The first one,

$$\delta G_{\mu\nu}^{(0)} = \kappa^{(0)}T_{\mu\nu} , \quad (\text{A12})$$

refers to a massless spin-2 field, with  $\delta G_{\mu\nu}^{(0)}$  perturbed Einstein tensor. The second set of solutions describes a massive theory whose equations of motions are given by

$$\delta G_{\mu\nu} = \kappa \left[ T_{\mu\nu} - \frac{\bar{g}_{\mu\nu}}{3}T \right] - \frac{\mu^2}{2}h_{\mu\nu} , \quad (\text{A13})$$

$$\nabla^\mu h_{\mu\nu} = \alpha \nabla_\nu T , \quad (\text{A14})$$

$$h = \alpha T , \quad (\text{A15})$$

where  $\delta G_{\mu\nu}$  is the first order perturbation of the Einstein tensor for a metric of the form  $g_{\mu\nu} = \bar{g}_{\mu\nu} + h_{\mu\nu}$ ,  $T_{\mu\nu}$  is the stress-energy tensor, to be considered as a first order perturbation of the background solution,  $h = g^{\mu\nu}h_{\mu\nu}$ ,  $T = g^{\mu\nu}T_{\mu\nu}$  and  $\kappa$ ,  $\alpha$  and  $\mu$  are constants, the latter depending on the parameters of the theory through

$$\mu^2 = M_v^4(c\beta_1 + 2c^2\beta_2 + c^3\beta_3) \left( \frac{1}{c^2M_f^2} + \frac{1}{M_g^2} \right) . \quad (\text{A16})$$

With a suitable choice of such constants,  $\kappa = 8\pi$  and  $\alpha = -\frac{2\kappa}{3\mu^2}$ , we obtain the equations of motion of a nonlinear spin-2 field with a linear mass term of mass  $\mu$ .

## Appendix B: Spherical decomposition of the metric tensor

In Sec. II we provide the master equations for all the components of the metric perturbation  $h_{\mu\nu}$

around the Schwarzschild solution. Due to the spherical symmetry of the background, the field  $h_{\mu\nu}$  can be expanded in term of a complete set of tensor spherical harmonics. The latter can be classified into *axial* and *polar* components, according to their properties under parity transformation [24, 25]. Axial modes change sign as  $(-1)^{\ell+1}$  under the inversion ( $\theta \rightarrow \pi - \theta, \phi \rightarrow \phi + \pi$ ), while polar perturbation are multiplied by a factor  $(-1)^\ell$ . The background spherical symmetry also yields a significant simplification of the formalism, as it leads the field's equations to be independent

of  $m$ , and does not allow perturbations with different multipole number, or different parity, to couple together.

In order to decompose the metric  $h_{\mu\nu}$ , and the test body stress-energy tensor  $T_{\mu\nu}$  in tensor spherical harmonics, we follow the approach introduced by Regge, Wheeler and Zerilli [24, 25]. As described in Sec. II, a generic tensor field can be expanded in terms of two classes of functions, the axial and polar harmonics. In this paper we have adopted the following ansatz for the metric perturbation  $\mathbf{h} = \mathbf{h}^{\text{ax}} + \mathbf{h}^{\text{pol}}$ , where<sup>3</sup>

$$\mathbf{h}^{\text{ax}} = \sum_{\ell m} \frac{\sqrt{2\ell(\ell+1)}}{r} \left[ i h_1^{\ell m}(r, t) \mathbf{c}_{\ell m} - h_0^{\ell m}(r, t) \mathbf{c}_{\ell m}^{(0)} + \frac{\sqrt{(\ell-1)(\ell+2)}}{2r} h_2^{\ell m}(r, t) \mathbf{d}_{\ell m} \right], \quad (\text{B1})$$

and

$$\begin{aligned} \mathbf{h}^{\text{pol}} = \sum_{\ell m} \left[ & f(r) H_0^{\ell m}(t, r) \mathbf{a}_{\ell m}^{(0)} - i\sqrt{2} H_1^{\ell m}(t, r) \mathbf{a}_{\ell m}^{(1)} + \frac{H_2^{\ell m}(t, r)}{f(r)} \mathbf{a}_{\ell m} - \frac{i}{r} \sqrt{2\ell(\ell+1)} \eta_0^{\ell m}(t, r) \mathbf{b}_{\ell m}^{(0)} \right. \\ & + \frac{1}{r} \sqrt{2\ell(\ell+1)} \eta_1^{\ell m}(t, r) \mathbf{b}_{\ell m} + \sqrt{\frac{l}{2}(\ell+1)(\ell-1)(\ell+2)} G^{\ell m}(t, r) \mathbf{f}_{\ell m} + \sqrt{2} K^{\ell m}(t, r) \mathbf{g}_{\ell m} \\ & \left. - \frac{\ell(\ell+1)}{\sqrt{2}} G^{\ell m}(t, r) \mathbf{g}_{\ell m} \right]. \end{aligned} \quad (\text{B2})$$

Similarly, we have decomposed the stress-energy tensor of the test particle as follows:

$$\begin{aligned} \mathbf{T} = \sum_{\ell=0}^{\infty} \sum_{m=-\ell}^{\ell} & \mathcal{A}_{\ell m}^{(0)} \mathbf{a}_{\ell m}^{(0)} + \mathcal{A}_{\ell m}^{(1)} \mathbf{a}_{\ell m}^{(1)} + \mathcal{A}_{\ell m} \mathbf{a}_{\ell m} \\ & + \mathcal{B}_{\ell m}^{(0)} \mathbf{b}_{\ell m}^{(0)} + \mathcal{B}_{\ell m} \mathbf{b}_{\ell m} + \mathcal{Q}_{\ell m}^{(0)} \mathbf{c}_{\ell m}^{(0)} + \mathcal{Q}_{\ell m} \mathbf{c}_{\ell m} \\ & + \mathcal{D}_{\ell m} \mathbf{d}_{\ell m} + \mathcal{G}_{\ell m} \mathbf{g}_{\ell m} + \mathcal{F}_{\ell m} \mathbf{f}_{\ell m}. \end{aligned} \quad (\text{B3})$$

The form of the axial ( $\mathbf{c}_{\ell m}^{(0)}, \mathbf{c}_{\ell m}, \mathbf{d}_{\ell m},$ ) and polar ( $\mathbf{a}_{\ell m}^{(0)}, \mathbf{a}_{\ell m}^{(1)}, \mathbf{a}_{\ell m}, \mathbf{b}_{\ell m}^{(0)}, \mathbf{b}_{\ell m}, \mathbf{g}_{\ell m}, \mathbf{f}_{\ell m}$ ) basis components are explicitly given in [26], while the expansion coefficients ( $\mathcal{A}_{\ell m}^{(0)}, \mathcal{A}_{\ell m}^{(1)}, \dots, \mathcal{F}_{\ell m}$ ) can be computed exploiting the orthonormality properties of the tensor harmonics:

$$(A, B) = \int \int \eta^{\mu\rho} \eta^{\nu\sigma} A_{\mu\nu}^* B_{\rho\sigma} d\Omega, \quad (\text{B4})$$

where the superscript  $\star$  denotes complex conjugation. Then, for example  $Q_{\ell m}^{(0)} = (\mathbf{c}_{\ell m}^{(0)}, \mathbf{T})$ . We refer the reader to Table 1 of [26] for the general expression of such coefficients.

Finally, we work in Fourier space, and decompose any function  $Z(t, r)$ , as

$$Z(t, r) = \frac{1}{\sqrt{2\pi}} \int_{-\infty}^{\infty} d\omega e^{-i\omega t} Z(\omega, r). \quad (\text{B5})$$

### Appendix C: Master equations for axial and polar perturbations

Having defined the decomposition of the metric and of the stress energy tensor, we can now derive the differential equations for the axial and polar perturbations ( $\mathbf{h}^{\text{ax}}, \mathbf{h}^{\text{pol}}$ ), numerically integrated in Sec. (III). The explicit form of such equations is provided for different multipole  $\ell$  in the next sections.

#### 1. Axial sector

$$a. \quad \ell \geq 2$$

A system of coupled differential equations for the three metric perturbations ( $h_0, h_1, h_2$ ) can be derived by replacing the anzatz (B2) within the linearized field's equations (A13)-(A15). Introduc-

<sup>3</sup> As noted in [6], we can not simplify eq. (B2) by imposing further gauge conditions, like those adopted by Regge and Wheeler [24], since they are too restrictive for the massive gravity theory considered in this work.

ing the new variables<sup>4</sup>  $Q(r) = h_1(r)(1 - 2M/r)$  and  $Z(r) = h_2(r)/r$ , the  $(r\theta)$  and  $(\theta\theta)$  components of eq. (A13) lead to the following Schrödinger-like equations for the axial sector,

$$\frac{d^2\boldsymbol{\Psi}}{dr_*^2} + [\omega^2 - V_{\text{ax}}] \boldsymbol{\Psi} = \mathcal{S}_{\text{ax}}, \quad (\text{C1})$$

where  $\boldsymbol{\Psi} = (Q, Z)^T$ , being  $r_* = r + 2M \ln(r/2M - 1)$  the tortoise coordinate. The potential matrix  $V_{\text{ax}}$  is given by,

$$V_{\text{ax}} = f \begin{bmatrix} \mu^2 + 2\frac{\lambda+3}{r^2} - \frac{16M}{r^3} & 2i\lambda\frac{3M-r}{r^3} \\ \frac{4i}{r^2} & \mu^2 + \frac{2\lambda}{r^2} + \frac{2M}{r^3} \end{bmatrix}, \quad (\text{C2})$$

$f(r) = 1 - 2M/r$ , and  $\lambda = \ell(\ell + 1)$ . The source term reads

$$\mathcal{S}_{\text{ax}} = \begin{bmatrix} \mathcal{S}_Q \\ \mathcal{S}_Z \end{bmatrix} = \frac{8\pi f(r)r}{\sqrt{\lambda + 1}} \begin{bmatrix} if(r)\mathcal{Q} \\ -\frac{\sqrt{2}}{\sqrt{\lambda}}\mathcal{D} \end{bmatrix}. \quad (\text{C3})$$

The coefficients  $\mathcal{Q}$  and  $\mathcal{D}$  represent the contribution of the infalling test particle, and depend on the specific orbital configuration considered. Their explicit form for radial plunge and circular motion is shown in appendix D.

Note also that the  $\theta$  component of eq. (A4) provides a first order differential equation for  $h_1$ , namely:

$$\frac{dh_1}{dr} = \frac{2(M-r)}{r^2 f(r)} h_1 - \frac{i\lambda}{r^2 f(r)} h_2 - \frac{i\omega}{f(r)^2} h_0, \quad (\text{C4})$$

which can be solved for  $h_0$ , once the solution for  $h_1$  and  $h_2$  has been obtained from eqns. (C1).

b.  $\ell = 1$

The metric perturbations for  $\ell = 0$  vanish identically in the axial sector, as  $\partial_\theta Y_{l,m} = \partial_\varphi Y_{l,m} = 0$ , and then the monopole term does not provide any contribution. For the dipole mode,  $\ell = 1$ , we are left with only two functions:  $h_0$  and  $h_1$ . A master equation for the latter can be derived from the  $(r\theta)$  component of eqns. (A13):

$$\frac{d^2Q}{dr_*^2} + [\omega^2 - V_{\text{Ax}}^{\ell=1}] Q = 8\pi ir f(r)^2 \mathcal{Q}. \quad (\text{C5})$$

where

$$V_{\text{Ax}}^{\ell=1} = f(r) \left( \frac{6}{r^2} - \frac{16M}{r^3} + \mu^2 \right), \quad (\text{C6})$$

and  $Q(r) = h_1(r)f$ . The function  $h_0$  is obtained again from eq. (C4), provided that  $h_2 = 0$ .

## 2. Polar sector

a.  $\ell \geq 2$

The procedure to obtain the fundamental relations for the polar sector follows the same spirit of the axial modes. The linearized field equations for the even parity metric lead in general to seven ODEs for the set of variables  $(H_0, H_1, H_2, \eta_0, \eta_1, K, G)$  (cfr. Appendix B). However, after some algebraic manipulations, it is possible to isolate a system of coupled equations for  $(G, K, \eta_1)$  only and, their first derivative  $(P, W, R) = d/dr_*(G, K, \eta_1)$ . Such system can be recast in a compact matrix form:

$$\left[ \frac{d}{dr_*} + V_{\text{pol}}^{\ell=2}(\omega, r) \right] \boldsymbol{\Xi} = \mathcal{S}_{\text{pol}}^{\ell=2}, \quad (\text{C7})$$

where  $\boldsymbol{\Xi} = (G, K, \eta_1, P, W, R)^T$ . The  $6 \times 6$  matrix potential  $V_{\text{pol}}^{\ell=2}$  depends on the frequency  $\omega$  and the mass  $\mu$ , as well as on the BH mass  $M$ . The actual expressions of  $V_{\text{pol}}^{\ell=2}$  and of the source vector  $\mathcal{S}_{\text{pol}}^{\ell=2}$  are rather cumbersome, and for sake of clarity we will not show them here, but they be explicitly reported within a `mathematica` notebook available at [27]. Finally, the  $(t, r, \theta)$  components of eqns. (A14) and the relation (A15), also provided in the supplementary material, yield four equations for  $(H_0, H_1, H_2, \eta_0)$  in terms of  $\boldsymbol{\Xi}$  and the test particle stress energy tensor, that can be solved after the solution of eqns. (C7) have been found.

b.  $\ell = 0$

The number of perturbations to be determined for the monopole mode in the even-parity sector decreases to four, i.e.  $(H_0, H_1, H_2, K)$ . We first use the time component  $\nabla^\mu h_{\mu t} = \alpha \nabla_t \delta T$  and the trace equation  $h = \alpha \delta T$  to eliminate  $H_0$  and  $H_2$ . We then proceed to replace their values in the  $(tt)$  and  $(tr)$  components of eq. (A13), as in the radial equation. From these, we obtain  $H_1$  and its first and second derivatives as function of  $K$  (and its derivatives also). Applying this to the  $(rr)$  component of eq. (A13) we obtain a 2<sup>nd</sup> order ODE for  $K$ . As noted in Sec. (II A), using the following change of variable

$$K = \frac{\sqrt{-4\mu^2 M + \mu^4 r^3 + 2\mu^2 r + 4r\omega^2}}{r^{5/2}} \varphi_0, \quad (\text{C8})$$

we obtain a wave equation for  $\varphi_0$  only:

$$\frac{d^2\varphi_0}{dr_*^2} + [\omega^2 - V_{\text{pol}}^{\ell=0}(r, \omega)] \varphi_0 = \mathcal{S}_{\text{pol}}^{\ell=0}. \quad (\text{C9})$$

For radial infall motion in the highly relativistic regime, the expression for  $\mathcal{S}_{\text{pol}}^{\ell=0}$  reduces to eq. (4).

<sup>4</sup> For the sake of clarity, hereafter we will neglect the  $(\ell, m)$  indices on the metric and source perturbations.

c.  $\ell = 1$

Finally, for the dipole term in the polar sector, the function  $G$  vanishes, and the perturbations are completely determined by two coupled equations for  $K$  and  $\eta_1$ , which can be derived, after some manipulations from the  $(tt)$  and  $(rr)$  components of eqns. (A13). It is possible to write the equations in a linear system:

$$\left[ \frac{d}{dr_*} + V_{\text{pol}}^{\ell=1}(r) \right] \boldsymbol{\Sigma} = \mathcal{S}_{\text{pol}}^{\ell=1}, \quad (\text{C10})$$

where  $\boldsymbol{\Sigma} = (K, \eta_1, dK/dr_*, d\eta_1/dr_*)^T$ , and  $V_{\text{pol}}^{(1)}$  is a  $4 \times 4$  potential matrix. Once the solution of the system is known, the remaining components of the metric  $(H_0, H_1, \eta_0, H_2)$  are obtained from the  $(rr)$  component of eqns. (A13), from the  $r$  and  $\theta$  terms of eqns. (A14), and from the trace of the metric perturbation (A15), respectively. The general expressions for the source terms are shown in the supplementary material, while in the highly relativistic head-on collisions, the vector  $\mathcal{S}_{\text{pol}}^{\ell=1}$  reduces to eqns. (6)-(7).

#### Appendix D: Components of the stress-energy tensor

In the case of radial plunge the form of the stress-energy tensor greatly simplifies. Moreover, the axial sector is not excited, as  $\mathcal{B}_{\ell m}^{(0)} = \mathcal{B}_{\ell m} = \mathcal{Q}_{\ell m}^{(0)} = \mathcal{Q}_{\ell m} = \mathcal{D}_{\ell m} = \mathcal{F}_{\ell m} = \mathcal{G}_{\ell m} = 0$ , and  $T_{\mu\nu}$  is given by

$$T_{\mu\nu}^{\ell m} = \begin{bmatrix} \mathcal{A}_{\ell m}^{(0)} & \frac{i}{\sqrt{2}} \mathcal{A}_{\ell m}^{(1)} & 0 & 0 \\ \frac{i}{\sqrt{2}} \mathcal{A}_{\ell m}^{(1)} & \mathcal{A}_{\ell m} & 0 & 0 \\ 0 & 0 & 0 & 0 \\ 0 & 0 & 0 & 0 \end{bmatrix} Y_{\ell m}(\theta, \varphi). \quad (\text{D1})$$

The non vanishing coefficients of the harmonic expansion then read:

$$\begin{aligned} \mathcal{A}_{\ell m}^{(0)} &= m_p u^0 \left( \frac{dr_p}{dt} \right)^{-1} \frac{f(r)^2}{r^2} e^{i\omega t_p} Y_{\ell m}^*(\theta_p, \varphi_p), \\ \mathcal{A}_{\ell m} &= m_p u^0 \frac{dr_p}{dt} \frac{e^{i\omega t_p}}{r^2 f(r)^2} Y_{\ell m}^*(\theta_p, \varphi_p), \\ \mathcal{A}_{\ell m}^{(1)} &= \sqrt{2} i m_p u^0 \frac{e^{i\omega t_p}}{r^2} Y_{\ell m}^*(\theta_p, \varphi_p), \end{aligned} \quad (\text{D2})$$

where  $u^0 = dt_p/d\tau = \gamma f(r)^{-1}$ ,  $dr_p/dt = -f(r)\gamma^{-1}\sqrt{\gamma^2 - f(r)}$ , and  $t_p = t_p(r)$  is a function of the radial orbital coordinate of the test body, that evolves according to

$$\frac{dt_p}{dr} = \left( \frac{dr_p}{dt} \right)^{-1} - \frac{\gamma f(r)^{-1}}{\sqrt{\gamma^2 - f(r)}}, \quad (\text{D3})$$

with  $\gamma$  being the particle's energy per unit mass (i.e., the Lorentz boost). Equation (D3) can be integrated together with the equations of the metric perturbations.

The procedure to compute the form of  $T_{\mu\nu}$  for circular orbits at a given radius  $\hat{r}$  is also straightforward. As in the Schwarzschild background geodesics are all planar, we can choose, without loss of generality, that  $\theta_p = \pi/2$ , and then

$$r_p(t) = \hat{r} \quad , \quad \varphi_p(t) = \omega_p t = \sqrt{\frac{M}{r^3}} t, \quad (\text{D4})$$

where  $\omega_p$  Keplerian frequency. The 4-velocity of the test particle reads

$$u^\mu = \left( \sqrt{\frac{r}{r-3M}}, 0, 0, \frac{1}{r} \sqrt{\frac{M}{r-3M}} \right). \quad (\text{D5})$$

For this configuration we have  $\mathcal{A} = \mathcal{A}^{(1)} = \mathcal{B} = \mathcal{Q} = \mathcal{F} = \mathcal{D} = 0$ , while the non vanishing coefficients of the expansion (B3) can be expressed in terms of the orbital parameters as follows:

$$\begin{aligned} \mathcal{A}_{\ell m}^{(0)} &= \frac{f(r)^2 m_p N_\ell}{\sqrt{2r^3(r-3M)}} P_{\ell m} \delta_\omega \delta_r, \\ \mathcal{B}_{\ell m}^{(0)} &= \frac{\sqrt{2} m_p f(r) \omega_p m N_\ell}{\sqrt{(\Lambda+1)r(r-3M)}} \delta_\omega \delta_r P_{\ell m}, \\ \mathcal{Q}_{\ell m}^{(0)} &= \frac{m_p f(r) \omega_p (1+\ell-m) N_\ell}{\sqrt{(\Lambda+1)\pi r(r-3M)}} \delta_\omega \delta_r P_{\ell+1 m}, \\ \mathcal{G}_{\ell m} &= \frac{m_p \omega_p^2 r N_\ell}{2\sqrt{r(r-3M)}} \delta_\omega \delta_r P_{\ell m}, \\ \mathcal{D}_{\ell m} &= \frac{m_p \omega_p^2 r (1+\ell-m) m N_\ell}{2\sqrt{\Lambda(\Lambda+1)r(r-3M)}} \delta_\omega \delta_r P_{\ell+1 m}, \\ \mathcal{F}_{\ell m} &= \frac{m_p \omega_p^2 r [2(\Lambda+1) - 2m^2] N_\ell}{\sqrt{2\Lambda(\Lambda+1)r(r-3M)}} \delta_\omega \delta_r P_{\ell m} \end{aligned} \quad (\text{D6})$$

Here,  $\delta_\omega \delta_r = \delta(\omega - m\omega_p) \delta(r - r_p)$ ,  $\Lambda = \frac{\ell(\ell+1)-2}{2}$ ,  $P_{\ell m}(\theta_p) = P_{\ell m}(\pi/2)$  are the Legendre polynomials, and  $N_\ell = \sqrt{(2\ell+1) \frac{(\ell-m)!}{(\ell+m)!}}$  is a normalization factor.

#### Appendix E: Numerical integration

In order to compute the metric perturbations produced by the infalling test particle, we need to solve the inhomogeneous equations derived in Sec. C1-C2. To this aim, we employ a Green function approach. We first consider a single second order equation of the form

$$\frac{d^2 \varphi}{dr_*^2} + (\omega^2 - V) \varphi = S, \quad (\text{E1})$$

as the one obtained for the monopole polar component (C9). The homogeneous problem associated to eq. (E1) is solved requiring that the solution satisfy purely ingoing waves at horizon and purely outgoing waves at spatial infinity. Let's assume that  $\varphi_{\pm}(\omega, r_*)$  are the two solutions of equation

$$\frac{d^2\varphi}{dr_*^2} + (\omega^2 - V)\varphi = 0$$

with boundary conditions

$$\lim_{r_* \rightarrow -\infty} \varphi_- \sim e^{-i\omega r_*}, \quad \lim_{r_* \rightarrow \infty} \varphi_+ \sim e^{k_\omega r_*}, \quad (\text{E2})$$

where  $k_\omega = \sqrt{V(r_* \rightarrow \infty) - \omega^2} = \sqrt{\mu^2 - \omega^2}$  is a complex quantity. For  $r_* \rightarrow \infty$  the  $\varphi_-$  component tends to the following analytical expression:

$$\lim_{r_* \rightarrow \infty} \varphi_- = \zeta(\omega)e^{k_\omega r_*} + \beta(\omega)e^{-k_\omega r_*}. \quad (\text{E3})$$

It can be shown that far from the source the general solution for the inhomogeneous equation (E1) can be constructed starting from  $\varphi_-(\omega, r_*)$  as

$$\varphi_{\text{out}}(\omega, r_*) = \frac{e^{k_\omega r_*}}{2k_\omega \beta(\omega)} \int_{-\infty}^{\infty} S(\omega, r_*) \varphi_-(\omega, r_*) dr_*,$$

with  $\omega^2 > V(r_* \rightarrow \infty)$ . This procedure can be generalized for a system of coupled differential equations, as those derived for the  $\ell = 1$  polar component [28]. For a given set of functions  $\Psi(r, \omega) = (\Psi_1, \dots, \Psi_n)$  that satisfy the linear system

$$\left[ \frac{d}{dr_*} + V \right] \Psi = \mathbf{S}, \quad (\text{E4})$$

with  $n$  source terms  $\mathbf{S} = (S_1, \dots, S_n)$ , the general solution is given by:

$$\Psi(r, \omega) = X \int_{-\infty}^{\infty} dr_* X^{-1} \mathbf{S}. \quad (\text{E5})$$

The fundamental matrix  $X$  contains  $2n$  independent solutions of the associated homogeneous problem which satisfy suitable boundary conditions, and that can be constructed as follows. At the horizon  $r_h$ , the proper solution has the following form:

$$\Psi(r_h) = \sum_{i=0}^N \mathbf{b}^{(i)}(r - r_h)^i e^{-i\omega r_*}, \quad (\text{E6})$$

where in general, the coefficients of the expansion depend on the form the leading vector  $\mathbf{b}^{(0)} = (b_1, \dots, b_n)$  only. The first  $n$  components of the matrix  $X$  can be obtained by choosing  $n$  initial conditions corresponding to  $\mathbf{b}_1^{(0)} = (1, 0, \dots, 0)$ ,

$\mathbf{b}_2^{(0)} = (0, 1, \dots, 0)$  and  $\mathbf{b}_n^{(0)} = (0, 0, \dots, 1)$ , and integrating the homogeneous equations *forward* from  $r_h$ . In the same way, at infinity, we ask the solution to satisfy the boundary condition given by

$$\Psi(r \rightarrow \infty) = \sum_{i=0}^N \mathbf{c}^{(i)} \frac{1}{r^i} r^\nu e^{k_\omega r_*}, \quad (\text{E7})$$

where  $\nu = M(k_\omega^2 - \omega^2)/k_\omega$  and again, the coefficients  $\mathbf{c}^{(i)}$  are all proportional to the  $i = 0$  terms only. Therefore, the remaining  $n$  component of the fundamental matrix can be constructed by specifying  $n$  linear independent vectors  $[c_1^{(0)} = (1, \dots, 0), \dots, c_n^{(0)} = (0, \dots, 1)]$  and integrating the homogeneous system *inward* down to the horizon. With this algorithm we can easily generate the components of  $X$  and then integrate eq. (E5).

As an example, for the  $\ell = 1$  circular motion described in Sec. II B, the linear system (E4) is defined in terms of metric functions  $K(\omega, r)$  and  $\eta_1(\omega, r)$ . In this case, the boundary conditions (E6)-(E7) are specified by two parameters  $(K^{(0)h}, \eta_1^{(0)h})$  and  $(K^{(0)\infty}, \eta_1^{(0)\infty})$  respectively. The matrix  $X$  can be then constructed by 4 solutions of eqns. (10). Two are obtained solving the ODEs from the horizon to infinity choosing the initial conditions as  $(K^{(0)h}, \eta_1^{(0)h}) = (1, 0)$  and  $(K^{(0)h}, \eta_1^{(0)h}) = (0, 1)$ . The other two can be derived integrating inward from infinity to the horizon with  $(K^{(0)\infty}, \eta_1^{(0)\infty}) = (1, 0)$  and  $(K^{(0)\infty}, \eta_1^{(0)\infty}) = (0, 1)$ . At the end we obtain:

$$X = \begin{bmatrix} K_h^{(1,0)} & K_h^{(1,0)} & K_\infty^{(1,0)} & K_\infty^{(0,1)} \\ \eta_h^{(1,0)} & \eta_h^{(1,0)} & \eta_\infty^{(1,0)} & \eta_\infty^{(0,1)} \\ K_h'^{(1,0)} & K_h'^{(1,0)} & K_\infty'^{(1,0)} & K_\infty'^{(0,1)} \\ \eta_h'^{(1,0)} & \eta_h'^{(1,0)} & \eta_\infty'^{(1,0)} & \eta_\infty'^{(0,1)} \end{bmatrix}, \quad (\text{E8})$$

where primes identify tortoise derivatives.

Once the numerical Fourier-domain solution is known, the gravitational waveform in the time domain is given by

$$\begin{aligned} \Psi(t) &= \int_{-\infty}^{\infty} \frac{\Psi^{\text{out}}(r, \omega) e^{-i\omega t}}{\sqrt{2\pi}} d\omega \\ &= \int_{-\infty}^{\infty} \frac{\mathbf{A}^{\text{out}}(\omega) e^{\sqrt{\mu^2 - \omega^2} r_*} e^{-i\omega t}}{\sqrt{2\pi}} d\omega, \end{aligned} \quad (\text{E9})$$

where  $\mathbf{A}^{\text{out}}(\omega)$  is the generic amplitude of the perturbation. Note that in order to compute the integral (E9) we need to specify an *extraction* radius, fixing  $r = R \gg r_h$ . The result of this approach is shown in Figs. 2-3 for the  $\ell = (0, 1)$  polar sector. The waveforms have been produced using two independent **Mathematica** codes, which yield the same output within the software numerical accuracy.

## Appendix F: The effective stress energy tensor

In this section we describe the basic equations to derive the explicit form of the GW luminosity for the dRGT theory. We first compute an effective stress-energy tensor  $T_{\mu\nu}^{\text{GW}}$  for the metric perturbations using the Noether theorem [29] applied to the the Lagrangian (A1), which reduces, in flat space-time, to the following expression:

$$\mathcal{L} = \frac{1}{64\pi} \left[ h_{\mu\nu,\lambda} h^{\mu\nu,\lambda} - 2h_{\mu\nu,\nu} h^{\mu\lambda,\lambda} + 2h_{\mu\nu,\nu} h^{\mu\mu} - h^{\mu} h_{,\mu} - 32\pi h_{\mu\nu} T^{\mu\nu} + \mu^2 (h_{\mu\nu} h^{\mu\nu} - h^2) \right],$$

such that

$$T_{\mu\nu}^{\text{GW}} = \left\langle \frac{\partial \mathcal{L}}{\partial h^{\alpha\beta,\mu}} h^{\alpha\beta,\nu} - \eta_{\mu\nu} \mathcal{L} \right\rangle.$$

Varying the Lagrangian, and using the field equations (A13)-(A15) to further simplify our calculations, we find

$$T_{\mu\nu}^{\text{GW}} = \frac{1}{32\pi} \langle h_{\alpha\beta,\mu} h^{\alpha\beta,\nu} - h_{,\mu} h_{,\nu} \rangle, \quad (\text{F1})$$

where angular brackets correspond to averaging on several wavelengths. The GW luminosity is then given by integrating the components  $T_{0i}^{\text{GW}}$ , that provide the energy which flows across the unit surface orthogonal to the axis  $x^i$  per unit time, i.e.,

$$\begin{aligned} L_{\text{GW}} &= \frac{dE}{dt} = \int T_{0i}^{\text{GW}} n^i r^2 d\Omega = \int T_{0r}^{\text{GW}} r^2 d\Omega \\ &= \frac{r^2}{32\pi} \int \langle h_{\alpha\beta,\mu} h^{\alpha\beta,\nu} \rangle d\Omega = \frac{r^2}{32\pi} \mathcal{C}_{\mu\nu}, \end{aligned} \quad (\text{F2})$$

where  $n^i = x^i/r$  is the unit vector specifying the normal to the surface element  $dS^i$ , and  $\mathcal{C}_{\mu\nu}$  is the angular average of the product of the metric perturbation derivatives. We can write the previous expression directly in the frequency domain. We first note that the generic perturbation  $h_{\alpha\beta}$  depends on the angular variables through the spherical harmonics of the multipole decomposition. Using the orthonormality properties of  $Y_{\ell m}(\theta, \phi)$  we can immediately perform the integral over the solid angle in eq. (F2). Moreover, using the Fourier transform (in cartesian coordinates):

$$\begin{aligned} h_{\alpha\beta}(\vec{x}, t) &= \frac{1}{\sqrt{2\pi}} \sum_{\ell,m} \int_{-\infty}^{\infty} d\omega e^{-i\omega t} h_{\alpha\beta}^{\ell m}(\vec{x}, \omega) \\ &\simeq \frac{1}{\sqrt{2\pi}r} \sum_{\ell,m} \int_{-\infty}^{\infty} d\omega e^{-i\omega t} e^{i\sqrt{\omega^2 - \mu^2}r} h_{\alpha\beta}^{\ell m}(\omega) \\ &= \sqrt{\frac{2}{\pi}} \frac{1}{r} \sum_{\ell,m} \Re \int_0^{\infty} d\omega e^{-i\omega t} e^{i\sqrt{\omega^2 - \mu^2}r} h_{\alpha\beta}^{\ell m}(\omega) \end{aligned}$$

where  $h_{\alpha\beta}^{\ell m} = h_{\alpha\beta}^{\text{ax},\ell m} + h_{\alpha\beta}^{\text{pol},\ell m}$ . We can now plug the former expressions into eq. (F2) and integrate over time, in order to compute the total emitted energy,

$$E = \frac{1}{16\pi} \sum_{\ell,m} \int_0^{\infty} d\omega [\mathcal{C}_{0r}^{\text{ax},\ell m} + \mathcal{C}_{0r}^{\text{pol},\ell m}] \omega \sqrt{\omega^2 - \mu^2},$$

and the GW energy spectrum,

$$\frac{dE}{d\omega} = \frac{1}{16\pi} \sum_{\ell,m} [\mathcal{C}_{0r}^{\text{ax},\ell m} + \mathcal{C}_{0r}^{\text{pol},\ell m}] \omega \sqrt{\omega^2 - \mu^2}, \quad (\text{F4})$$

where,

$$\begin{aligned} \mathcal{C}_{0r}^{\text{pol},\ell m} &= |H_0(\omega)|^2 - 2|H_1(\omega)|^2 + |H_2(\omega)|^2 - \frac{2\lambda}{r^2} |\eta_0(\omega)|^2 \\ &\quad + \frac{2\lambda}{r^2} |\eta_1(\omega)|^2 + \frac{1}{2} \lambda(\lambda-1) |G(\omega)|^2 + 2|K(\omega)|^2 \\ &\quad - \lambda(K^*(\omega)G(\omega) + G^*(\omega)K(\omega)) \\ \mathcal{C}_{0r}^{\text{ax},\ell m} &= -\frac{2\lambda}{r^2} |h_0(\omega)|^2 + \frac{2\lambda}{r^2} |h_1(\omega)|^2 + \frac{\lambda(\lambda-2)}{2r^2} |h_2(\omega)|^2. \end{aligned}$$

For the polar  $\ell = 0$  case, shown in Fig. 1, we simply have:

$$\frac{dE^{\ell=0}}{d\omega} = \frac{3}{8\pi} \frac{|\varphi_0(\omega)|^2}{\omega} \omega \sqrt{\omega^2 - \mu^2} \mu^4. \quad (\text{F5})$$

As described in Sec. C 2 c, for the dipolar mode, the metric perturbations are completely determined by  $K$  and  $\eta_1$ . The remaining variables  $(H_0, H_1, \eta_0, H_2)$  are therefore determined in terms of the formers, once the numerical solution is known. Substituting these expressions within eq. (F4) we find the energy spectrum of the  $\ell = 1$  mode in the radial infall case:

$$\begin{aligned} \frac{dE^{\ell=1}}{d\omega} &= \frac{\omega \sqrt{\omega^2 - \mu^2}}{16\pi} \left( 2|K|^2 + 4\frac{\mu^2}{\omega^2} |\eta_1|^2 \right. \\ &\quad \left. + 9|K + \eta_1|^2 + \left( 2\frac{\mu^2}{\omega^2} - 1 \right) |K + 3\eta_1|^2 \right). \end{aligned} \quad (\text{F6})$$

For circular orbits, we have also computed the luminosity  $dE/dt$ . The computation in this case is straightforward, as the source terms of the field's equations depend on  $\delta(\omega - \omega_p)$ , where  $\omega_p = m\sqrt{M/r_p^3}$  is the Keplerian frequency of the test particle on the equatorial orbit specified by the radius  $r_p$  (see Sec. D). Therefore, we can write the generic perturbation as  $h_{\alpha\beta}^{\ell m}(r, \omega) = \bar{h}_{\alpha\beta}^{\ell m}(r, \omega) \delta(\omega - m\omega_p)$ , and integrate the Dirac's delta in eq. (F3). Replacing this expression into the GW luminosity (F2), and averaging over several periods, we finally obtain the energy per unit time emitted by the sys-

tem, with a test-body on circular geodesics,

$$\frac{dE}{dt} = \frac{1}{16\pi} \sum_{\ell,m} \sum_{\alpha,\beta=0}^4 \left( |\bar{h}_{\alpha\beta}^{\text{ax},\ell m}(\omega_p)|^2 + |\bar{h}_{\alpha\beta}^{\text{pol},\ell m}(\omega_p)|^2 \right) \omega_p \sqrt{\omega_p^2 - \mu^2}. \quad (\text{F7})$$

Again, the  $\ell = 1$  component is explicitly given by

$$\frac{dE^{\ell=1}}{dt} = \frac{\omega_p \sqrt{\omega_p^2 - \mu^2}}{32\pi^2} (2|\bar{K}|^2 + 4\mu^2/\omega^2|\bar{\eta}_1|^2 + 9|\bar{K} + \bar{\eta}_1|^2 + (2\mu^2/\omega_p^2 - 1)|\bar{K} + 3\bar{\eta}_1|^2). \quad (\text{F8})$$

---

[1] E. Berti *et al.*, *Class. Quant. Grav.* **32**, 243001 (2015), arXiv:1501.07274 [gr-qc].

[2] L. Barack *et al.*, (2018), arXiv:1806.05195 [gr-qc].

[3] K. Hinterbichler, *Rev. Mod. Phys.* **84**, 671 (2012), arXiv:1105.3735 [hep-th].

[4] C. de Rham, *Living Rev. Rel.* **17**, 7 (2014), arXiv:1401.4173 [hep-th].

[5] C. M. Will, *Phys. Rev.* **D57**, 2061 (1998), arXiv:gr-qc/9709011 [gr-qc].

[6] R. Brito, V. Cardoso, and P. Pani, *Phys. Rev.* **D88**, 023514 (2013), arXiv:1304.6725 [gr-qc].

[7] L. S. Finn and P. J. Sutton, *Phys. Rev.* **D65**, 044022 (2002), arXiv:gr-qc/0109049 [gr-qc].

[8] V. Cardoso, L. Gualtieri, C. Herdeiro, and U. Sperhake, *Living Rev. Relativity* **18**, 1 (2015), arXiv:1409.0014 [gr-qc].

[9] U. Sperhake, C. J. Moore, R. Rosca, M. Agathos, D. Gerosa, and C. D. Ott, *Phys. Rev. Lett.* **119**, 201103 (2017), arXiv:1708.03651 [gr-qc].

[10] R. Brito, V. Cardoso, C. F. B. Macedo, H. Okawa, and C. Palenzuela, *Phys. Rev.* **D93**, 044045 (2016), arXiv:1512.00466 [astro-ph.SR].

[11] E. Barausse, N. Yunes, and K. Chamberlain, *Phys. Rev. Lett.* **116**, 241104 (2016), arXiv:1603.04075 [gr-qc].

[12] V. Cardoso, S. Chakrabarti, P. Pani, E. Berti, and L. Gualtieri, *Phys. Rev. Lett.* **107**, 241101 (2011), arXiv:1109.6021 [gr-qc].

[13] N. Yunes, P. Pani, and V. Cardoso, *Phys. Rev.* **D85**, 102003 (2012), arXiv:1112.3351 [gr-qc].

[14] R. Fujita and V. Cardoso, *Phys. Rev.* **D95**, 044016 (2017), arXiv:1612.00978 [gr-qc].

[15] E. Babichev and A. Fabbri, *Class. Quant. Grav.* **30**, 152001 (2013), arXiv:1304.5992 [gr-qc].

[16] R. Brito, V. Cardoso, and P. Pani, *Phys. Rev.* **D88**, 064006 (2013), arXiv:1309.0818 [gr-qc].

[17] M. S. Volkov, in *Proceedings, 14th Marcel Grossmann Meeting on Recent Developments in Theoretical and Experimental General Relativity, Astrophysics, and Relativistic Field Theories (MG14) (In 4 Volumes): Rome, Italy, July 12-18, 2015*, Vol. 2 (2017) pp. 1779–1798, arXiv:1601.08230 [gr-qc].

[18] R. A. Rosen, *JHEP* **10**, 206 (2017), arXiv:1702.06543 [hep-th].

[19] C. de Rham, G. Gabadadze, and A. J. Tolley, *Phys. Rev. Lett.* **106**, 231101 (2011), arXiv:1011.1232 [hep-th].

[20] S. F. Hassan, A. Schmidt-May, and M. von Strauss, *Journal of High Energy Physics* **2013**, 150 (2013).

[21] V. Baccetti, P. Martin-Moruno, and M. Visser, *Class. Quant. Grav.* **30**, 015004 (2013), arXiv:1205.2158 [gr-qc].

[22] C. de Rham and G. Gabadadze, *Phys. Rev.* **D82**, 044020 (2010), arXiv:1007.0443 [hep-th].

[23] S. F. Hassan, A. Schmidt-May, and M. von Strauss, *JHEP* **05**, 086 (2013), arXiv:1208.1515 [hep-th].

[24] T. Regge and J. A. Wheeler, *Physical Review* **108**, 1063 (1957).

[25] F. J. Zerilli, *Physical Review D* **2**, 2141 (1970).

[26] N. Sago, H. Nakano, and M. Sasaki, *Physical Review D* **67**, 3457 (2003).

[27] <https://centra.tecnico.ulisboa.pt/network/grit/files/>.

[28] P. Pani, V. Cardoso, and L. Gualtieri, *Physical Review D* **83**, 3 (2011).

[29] L. S. Finn and P. J. Sutton, *Physical Review D* **65**, 1159 (2002).